

## Effect of hydroxyapatite nanoparticles on structural and electrical properties of ethylene propylene diene monomer rubber

A. Nihmath and M. T. Ramesan\*

Department of Chemistry, University of Calicut, Calicut University P.O., Kerala, India 673 635

\*Corresponding author: E-Mail: [mtramesan@uoc.ac.in](mailto:mtramesan@uoc.ac.in)

### ABSTRACT

In this article, hydroxyapatite nanoparticles (HA) supported on ethylene propylene diene monomer (EPDM) rubber have been prepared and characterized. Nanocomposites of EPDM with HA nanoparticles were prepared by mechanical mixing in a two roll mill in presence of dicumyl peroxide (DCP) as crosslinking agent. The structural reorganization of nanocomposite was studied by FTIR, UV-Visible spectroscopic techniques and XRD. Spectroscopic studies revealed that the incorporation of nanoparticles into the elastomer leads to an interfacial interaction between the nanoparticles and polymer. The XRD analysis ascertained the presence of HA nanoparticles in the EPDM chain. Optical and scanning electron microscopy was conducted to characterize the dispersion of nanoparticle inside the macromolecular chain of EPDM. The changes in thermal behaviour of EPDM rubber was characterized by TGA and DSC. The thermal stability and glass transition temperature of nanocomposites were increased with the increase in weight percentage of HA nanoparticles. The AC electrical conductivity and dielectric constant of nanocomposite were found to be increases with the increase in concentration of nanoparticles.

**KEY WORDS:** EPDM, nano-hydroxyapatite, nanocomposite, crystallinity, thermal properties, electrical properties.

### 1. INTRODUCTION

Ethylene propylene diene monomer (EPDM) rubber is a well known general purpose elastomer having versatile utilization in material industry ranging from automotive to household application. Particular attention has been focused on EPDM rubber because of their unique characteristics such as outstanding ozone and heat resistance, weathering ability, aging properties etc. due to stable saturated hydrocarbon chains with low percentage of olefinic side chains (Seo, 2011). But the thermodynamic immiscibility results high interfacial tension due to the lack of polarity, limits its application in engineering fields. To overcome this difficulty, recently many research works were carried out on EPDM by making use of its ability to respond high filler loading due to the presence of high ethylene content (Bhadane, 2006; El-Wakil, 2011).

The nanocomposite with large interfacial area per unit volume shows better mechanical, electrical, thermal performance (Ramesan, 2013, Ramesan, 2014; Tae, 2002). EPDM based nanocomposites have got great research interest. The nanocomposites of polymer with ceramic material as filler have the merits of both polymer and ceramic. The nano sized hydroxyapatite is one of the most studied bio ceramic materials which have excellent biodegradability, biocompatibility and osteoconductive properties (Chen, 2002). Polyamide /hydroxyapatite nanocomposite with greater biocompatibility and mechanical strength was prepared by Li (2010). Though polypropylene is a bioinert polymer, its nanocomposite with HA shows bioactive characteristics, dimensional stability and high mechanical strength (Liao, 2013). Further, literature reports point out the use of polymeric ceramic nanocomposites as energy storage materials because of the low temperature processability of polymer and high dielectric constant of ceramics (Siddabattuni and Schuman, 2014). The present work report on the preparation of EPDM/HA nanocomposite with different loading of synthesized hydroxyapatite nanoparticles. The structural characterization of the prepared nanocomposite was studied by FTIR and UV-VIS spectroscopy, XRD, TGA and DSC. Optical microscopy and SEM were used to analyze the morphological characteristics. Furthermore, the AC conductivity and the dielectric properties of nanocomposite were also investigated.

### 2. MATERIALS AND METHODS

EPDM-502 was obtained from Herdillia Unimers Ltd. (Mumbai, India). The analytical grade  $\text{CaCl}_2$ ,  $(\text{NH}_4)_2\text{HPO}_4$ ,  $\text{NH}_4\text{OH}$  were used for the synthesis of nano hydroxyapatite. The cross linking agent used was commercial grade dicumyl peroxide (DCP) obtained from local rubber chemical suppliers.

**2.1. Synthesis of Hydroxyapatite nanoparticle:** Hydroxyapatite nanoparticles were prepared by chemical precipitation method as described earlier (Pang, 2003). Typically, equimolar concentration of  $\text{CaCl}_2$  and  $(\text{NH}_4)_2\text{HPO}_4$  were prepared in an aqueous solution and these solutions were preheated, mixed under vigorous stirring.  $\text{NH}_4\text{OH}$  was added to the reaction mixture immediately after mixing until the pH reached to 10. After stirring for 24 hours the precipitate was filtered, washed with water and dried and the HA powder was then sintered at  $600^\circ\text{C}$  for 6hrs.

**2.2. Preparation of EPDM/HA nanocomposite:** EPDM/HA nanocomposites were prepared by adding various amount of hydroxyapatite nanoparticles in an open two roll mill mixing technique. Rubber (100phr) is mixed with curing agent DCP (6phr) and HA nanoparticles (5, 10, 15 and 20 phr). The samples were vulcanized to their respective cure time in hydraulic press at 160°C. For comparison a blank compound was also prepared by mixing EPDM and DCP.

**2.3. Characterization:** The IR spectra of the composites were recorded on a JASCO (model 4100) Fourier transform infrared spectrophotometer in the region 500–4000  $\text{cm}^{-1}$ . The UV spectra of samples were obtained using a Hitachi U-300 spectrophotometer. X-ray diffraction pattern of the sample was recorded on Philips X-ray diffractometer using  $\text{CuK}\alpha$  radiation ( $\lambda = 1.5406 \text{ \AA}$ ). The diffractogram was recorded in terms of  $2\theta$  in the range  $10^\circ$ – $80^\circ$ . The optical images of composites were taken by using Trinocular microscope Model Axio Lab. A1 attached Axio Cam ERc5s Carl Zeiss Micro imaging GmbH Analyzer. The surface morphology of the rubber was investigated by using Field Emission Scanning Electron Microscopy (FESCA)-Hitachi, SU 6600 (FESEM). Thermal decomposition behaviour of the nanocomposite was investigated by a Perkin Elmer thermo gravimetric analyzer at a heating rate of  $10^\circ\text{C}/\text{min}$  in a dry nitrogen atmosphere. DSC analysis was carried out by Mettler Toledo DSC 22e at a heating rate of  $5^\circ\text{C}/\text{min}$  (atmosphere  $\text{N}_2$ ; flow 40 ml/min). AC resistivity and Dielectric constant of the samples was measured by Hewlett–Packard LCR meter, in a frequency range 100– $10^6$  Hz at room temperature.

### 3. RESULTS AND DISCUSSION

**3.1. FT-IR Characterization:** Fourier transform infrared spectrum is used to determine the composition of the prepared EPDM/HA nanocomposites. The IR spectra of EPDM with different concentration of nanoparticles are given in Figure 1. The hydroxyapatite shows O-H stretching vibration at  $3573 \text{ cm}^{-1}$  and O-H bending mode at  $633 \text{ cm}^{-1}$ . Also, the IR absorption at 964,  $1045 \text{ cm}^{-1}$  are assigned to the P-O-stretching vibration of  $(\text{PO}_4)^{3-}$  group and the peaks obtained at 633, 602 and  $568 \text{ cm}^{-1}$  are corresponding to its bending vibration (Nejati, 2009). The pristine EPDM shows absorption peaks at  $1157 \text{ cm}^{-1}$ ,  $1457 \text{ cm}^{-1}$  and  $2904 \text{ cm}^{-1}$  corresponding to C-H stretching vibration of polypropylene segment and the peak at  $721 \text{ cm}^{-1}$  which is attributed to side ethyl groups of crystalline ethylene blocks (Vilsan, 2015). The nanocomposite contains most of the absorption bands present in the EPDM and HA along with a slight shift in absorption frequency. The OH stretching is shifted from  $3573 \text{ cm}^{-1}$  to  $3568 \text{ cm}^{-1}$  and bending vibration is changed from  $633 \text{ cm}^{-1}$  to  $638 \text{ cm}^{-1}$ . Furthermore, an absorption band is present in nanocomposite (at  $1022$ – $1164 \text{ cm}^{-1}$ ) may be due to the combination of C-H stretching vibration of polypropylene in EPDM ( $1157 \text{ cm}^{-1}$ ) and  $\text{PO}_4^{3-}$  entity ( $1045 \text{ cm}^{-1}$ ) of HA. These results assure the incorporation of nano-HA in EPDM rubber.

**3.2. UV-VIS Spectroscopy:** The diffuse reflectance UV-VIS spectra scanned at 200–600 nm of EPDM and EPDM/HA nanocomposite is given in Figure 2. Hydroxyapatite nanoparticle shows an absorption maximum at 263 nm and a dip at 421 nm. EPDM shows a broad absorption band with absorption maxima at 347 nm. The chromophore responsible for initial UV light absorption is the carbon-carbon double bond present in EPDM. It is very clear from the figure that the nanocomposites also show a maximum absorption of UV light below 300 nm and an absorption dip in 300–400 nm range which reflects the successful introduction of nano-apatite particles in to the matrix. Moreover, the absorption maximum in the nanocomposite shows a shift to higher energy region than that of EPDM. This hypochromic shift may be due to the interfacial interaction of HA and the chains of EPDM.

**3.3. X-Ray Diffraction Analysis:** The X-ray diffraction patterns of EPDM and EPDM / HA nanocomposite with different concentration of nanoparticle is given in Figure 3. Being a crystalline bioceramic hydroxyapatite nanoparticle shows  $2\theta$  values at  $25.7^\circ$ ,  $31.6^\circ$ ,  $32.7^\circ$ ,  $34.1^\circ$ ,  $39.7^\circ$ ,  $46.6^\circ$ ,  $49.5^\circ$  and  $53.09^\circ$  corresponding to the crystal planes 002, 211, 300, 202, 310, 222, 213, 321 and 004 (Arsad, 2011). EPDM shows an intense broad diffraction peak at  $2\theta = 17.8^\circ$  indicating its amorphous nature and a small peak at  $2\theta = 28^\circ$ . This small sharp crystalline peak may be due to the presence of side ethylene of polyethylene block. From the plots it is very clear that nanocomposite exhibit very few crystalline peaks of HA with decrease in intensity. The crystalline peak corresponding to polyethylene segment of EPDM is absent in nanocomposite and also a new diffraction peak appeared at  $2\theta = 31^\circ$ . It is interesting to see that the amorphous region of the composite is shifted to a lower  $2\theta$  region with 20 phr HA nanoparticles. In addition to this the intensity of amorphous and crystalline peaks decreases with increase in the dosage of nanoparticles. This proves that the efficient interfacial interaction between the elastomer and the ceramic occurs at lower loading of nanoparticles. At higher loading of HA, the variation in amorphous and crystalline region of nanocomposite is attributed to the agglomeration of nanoparticles which is in good agreement with the optical micrographs.

**3.4. Morphological Studies:** The distribution of nanoparticle in EPDM matrix is examined by SEM and optical microscopy. The SEM image of EPDM with 10 phr HA nanoparticle is presented in Figure 4. It depicts the spherically shaped clusters of nano HA in the host rubber. The dispersed particles are agglomerated due to the self aggregation through strong polar attraction between OH groups within nonpolar macromolecular system.

Figure 5 demonstrates the optical micrographs of EPDM and its nanocomposites with HA. EPDM shows homogenous smooth surface whereas in nanocomposite at lower concentration of nanoparticle (5 phr) shows almost uniform distribution of filler loading. Thus the micrograph point out the good adhesion between nano filler and the polymer matrix.

**3.5. Thermogravimetric Analysis (TGA):** Thermogravimetric analysis of newly prepared nanocomposite presented in Figure 6 shows single stage decomposition. The degradation temperature of EPDM chain is at 434°C whereas the decomposition temperature increases as the concentration of nanoparticle increases. That is EPDM with 5 phr HA shows decomposition at 438°C while EPDM/ 15 phr HA degrades at 445°C. The elevation in decomposition temperature clearly indicates the improved thermal stability of nanocomposite which is due to the nanoparticle penetrated in to the EPDM reduces the diffusion of oxygen in to the long chain of elastomer. Besides, the char residue obtained at 600°C for EPDM is 1.2% whereas the nanocomposites with 5 and 15 phr HA are about 4.7% and 9.3 % respectively. The increase in percentages of final char residue with the increase in filler loading indicates that the nanoparticles act as heat barrier to EPDM and thus enhances the flame retardancy of rubber (Nihmath and Ramesan, 2014).

**3.6. Differential Scanning Calorimetry (DSC):** DSC analysis was performed to determine the glass transition temperature (T<sub>g</sub>) of fabricated nanocomposite. The T<sub>g</sub> obtained as base line shift in thermograms are shown in Figure 7 for EPDM and its nanocomposites with HA. The EPDM shows T<sub>g</sub> at -53°C, the nanocomposite with 5 and 15 weight % HA are present at -51°C and -48°C respectively. The raise in T<sub>g</sub> of newly prepared EPDM/HA nanocomposites is attributed to the intermolecular interaction through the enhanced interface of nanocomposite which restricts the rotational motion within the chains. Also, the incorporation of HA increases the compactness of the system as evident from the XRD resulting in the reduction of free volume inside the composite which in turn suppresses the motion of polymer chains (Ramesan, 2014 a).

### 3.7. Conductivity Studies

**3.7.1. AC Conductivity:** The AC electrical conductivity as a function of frequency of EPDM and EPDM with different content of HA nanoparticles are depicted in Figure 8. The conductivity goes on increasing with frequency which is due to the hopping of charge carriers through the conducting networks formed as a result of polarity induced by the hydroxyl group of hydroxyapatite to the EPDM chains. Further, the electrical conductivity of nanocomposite is better than neat EPDM and the conductivity increases proportionately with increase in concentration of HA. It can be explained on the microscopic conductivity arising from the matrix-filler interaction, polarity and chain entanglements in the host matrix (Ramesan, 2014 b). As it is revealed from XRD studies the crystallinity of EPDM increases with the incorporation of nano HA resulting in the improvement of orderness through the interconnection of dispersed filler and the rubber matrix. It can also be seen from the graph that the conductivity of nanocomposite with 20phr HA is less than that of nanocomposite with 15phr HA due to aggregation of nanoparticle at higher loading (Ramesan, 2015).

**3.7.2. Dielectric Constant:** The dielectric constants of the composites are portrayed in Figure 9. It can be observed that dielectric constant shows frequency independent behaviour at high frequency and strong distortion of permittivity at lower frequency region and also the dielectric constant increases with the concentration of nano-HA. At lower frequencies the interfacial polarization raised by the introduction of polar filler into the rubber matrix is the reason for high dielectric constant while at higher frequencies the orientation polarization plays important role (Anil and Ramesan, 2014). That is up to about 10<sup>3</sup>Hz the AC current is in phase with the applied potential whereas above 10<sup>3</sup>Hz the filler aggregates do not get enough time for hoping before the reversal of the field. As the filler concentration increases the electrical polarization of the elastomer matrix increases due to the presence of more number of polar hydroxyl groups.

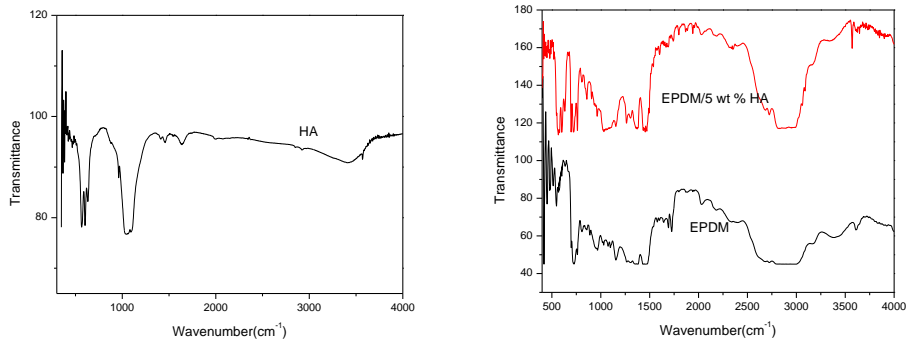


Figure.1. FTIR spectra of EPDM, HA and EPDM/5 phr HA

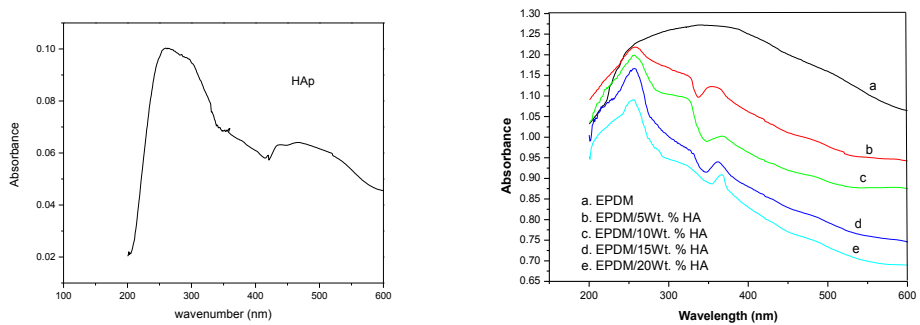


Figure.2. UV spectra of HA and EPDM/HA nanocomposites

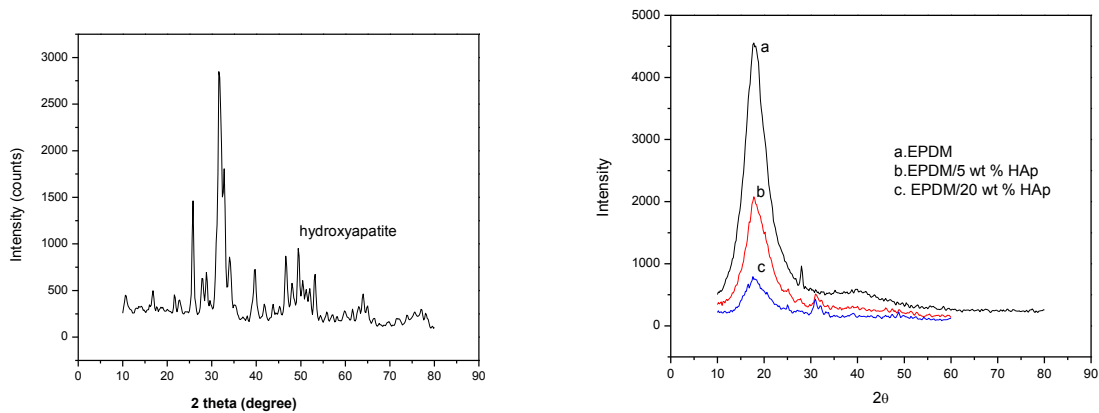


Figure.3. XRD pattern of HA, EPDM and EPDM/HA nanocomposites

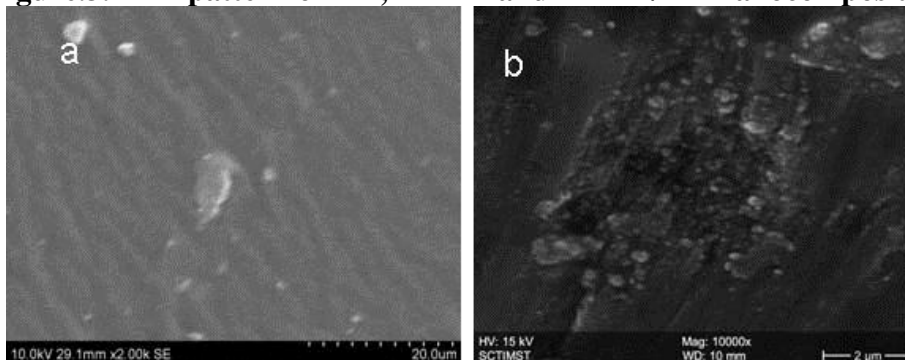


Figure. 4. SEM images of EPDM and EPDM/10phr HA

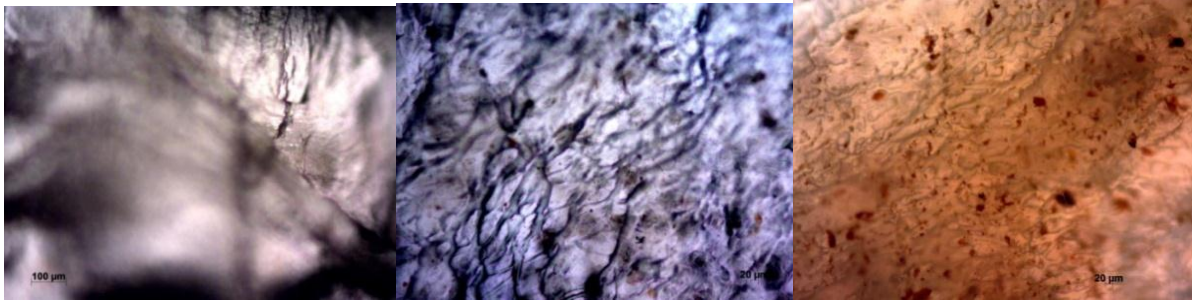


Figure 5. Optical micrographs of a) EPDM b) EPDM/5 phr HA c) EPDM/15phr HA

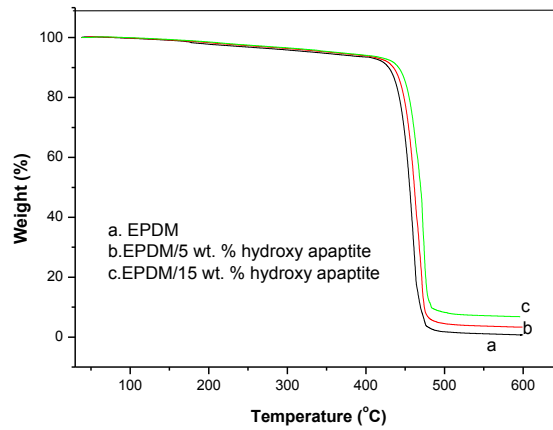


Figure.6.TGA thermograms of EPDM and EPDM/HA nanocomposites

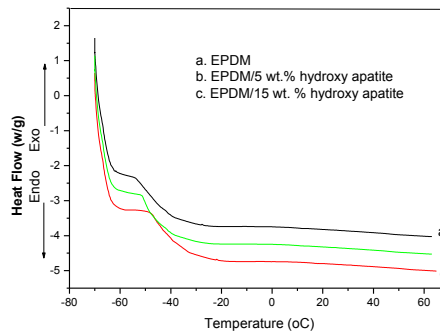


Figure.7.DSC thermograms of EPDM and EPDM/HA nanocomposites

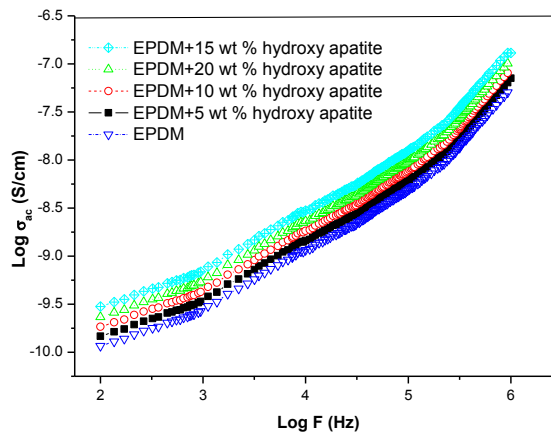
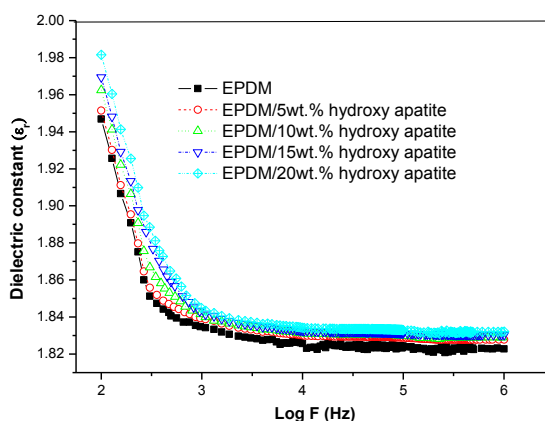


Figure.8. AC conductivity of EPDM and EPDM/HA nanocomposites



**Figure.9. Dielectric constant of EPDM and EPDM/HA nanocomposites**

#### 4. CONCLUSIONS

Hydroxyapatite nanoparticles (HA) was synthesized by the chemical precipitation between  $\text{CaCl}_2$  and  $(\text{NH}_4)_2\text{HPO}_4$  in aqueous solution. EPDM/HA nanocomposite was prepared by simple two roll mill mixing method in presence of dicumyl peroxide as crosslinking agent. The effect of hydroxy apatite nanoparticles on EPDM rubber was studied and characterized by FTIR, UV, XRD, TGA, DSC and electrical conductivity measurements. FT-IR spectra indicated the incorporation of hydroxyapatite with the elastomer chain. UV-Visible spectroscopy confirms the enhanced interfacial interaction of nanoparticles and the elastomeric chain. XRD pattern of composite showed few diffraction peak of HA in the polymer matrix. The intercalation and flocculation of inorganic nanoparticles in organic matrix can be revealed from optical micrographs and also from SEM images. The thermal behaviour of newly prepared nanocomposite increased with increase in concentration of nanoparticles. DSC analysis showed better the glass transition temperature of nanocomposite was higher than neat EPDM and the  $T_g$  increases with increase in content of nanoparticles in the polymer, indicating the interfacial interaction between matrix and the nanoparticles. The EPDM/HA nanocomposite with higher weight percentage of HA nanoparticle shows higher AC conductivity than pristine rubber due to the improved interconnection between nanoparticle and polymer that result in an ordered arrangement of filler inside the macromolecular chain of EPDM. Dielectric constant of nanocomposite exhibit similar behaviour to the applied frequency and was significantly increased with increase in concentration of HA nanoparticles.

#### 5. ACKNOWLEDGMENTS

Authors are thankful to Dr.P.P.Pradyumnan, Department of Physics, University of Calicut for the conductivity and XRD studies. The authors also wish to acknowledge University Grants Commission, New Delhi for their financial assistance.

#### REFERENCES

- Anilkumar T, Ramesan MT, Synthesis and electrical conductivity studies of metal chloro and nitroxide group containing styrene butadiene rubber, American Institute of Physics Conference Proceedings, 1620, 2014, 28-34.
- Arsad MSM, Lee PM., Hung LK, Synthesis and characterization of hydroxyapatite nanoparticles and  $\beta$ -TCP particles, 2<sup>nd</sup> International Conference on Biotechnology and Food Science IPCBEE, 7, 2011, 184-188.
- Bhadane P, Champagne M, Huneault M, Tofan F, Favis B, Continuity development in polymer blends of very low interfacial tension, Polymer, 47, 2006, 2760-2771.
- Chen F, Wang ZC, Lin CJ, Preparation and characterization of nano-sized hydroxyapatite particles and hydroxyapatite/chitosan nano – composite for use in biomedical materials, Material Letters, 57, 2002, 858–861.
- El-Wakil AA, Enhancement of adhesion between EPDM and polyester fabric by using NR modified maleic anhydride, International Journal of Polymer Science, 2011, 2011, 1-4.
- Li J, Li Y, Ma S, Gao Y, Zuo Y, Hu J, Enhancement of bone formation by BMP-7 transduced MSCs on biomimetic nano-hydroxyapatite/polyamide composite scaffolds in repair of mandibular defects, Journal of Biomedical Materials Research Part A, 95, 2010, 973-81.

Liao CZ, Li K, Wong HM, Tong WY, Yeung KWK, Tjong SC, Novel polypropylene biocomposites reinforced with carbon nanotubes and hydroxyapatite nanorods for bone replacements, *Materials Science and Engineering: C*, 33, 2013,1380-1388.

Nejati E, Firouzdar V, Eslaminejad MB, Bagheri F, Needle-like nano hydroxyapatite/poly (L-lactide acid) composite scaffold for bone tissue engineering application, *Materials Science and Engineering: C*, 29, 2009, 942–949.

Nihmath A, Ramesan MT, Development, characterization and conductivity studies of chlorinated EPDM, *American Institute of Physics Conference Proceedings*, 1620, 2014, 353-359.

Pang YX, Bao X, Influence of temperature, ripening time and calcination on the morphology and crystallinity of hydroxyapatite nanoparticles, *Journal of the European Ceramic Society*, 23, 2003, 1697–1704.

Ramesan MT, Dynamic mechanical properties, magnetic and electrical behavior of iron oxide/ ethylene vinyl acetate nanocomposites, *Polymer Composites*, 35, 2014 b, 1989-1996.

Ramesan MT, Effect of fly ash on thermal stability, flammability, oil resistance and transport properties of chlorinated styrene butadiene rubber composites, *Journal of Elastomers and Plastics*, 46, 2014 a, 303-324.

Ramesan MT, Nihmath A, Francis J, Preparation and characterization of zinc sulphide nanocomposites based on acrylonitrile butadiene rubber, *American Institute of Physics Conference Proceedings*, 1536, 2013, 255-256.

Ramesan MT, Processing characteristics and mechanical and electrical properties of chlorinated styrene butadiene rubber/ fly ash composites, *Journal of Thermoplastic Composite Materials*, 28, 2015, 286-1300.

Ramesan MT, Synthesis and characterization of magnetoelectric nanomaterial composed of Fe<sub>3</sub>O<sub>4</sub> and polyindole, *Advances in Polymer Technology*, 32, 2013, 928-934.

Seo YD, Lee HS, Kim YS, Song C, A study on the aging degradation of EPDM under local condition, *Nuclear Engineering and Technology*, 43, 2011,279-286.

Siddabattuni S, Schuman TP, Polymer composites for energy harvesting, conversion, and storage, 1161, *ACS Symposium Series*, American Chemical Society, Washington DC, 2014, 165–190.

Tae HK, Lee WJ, Dong CL, Hyoungh JC, John MS, Synthesis and rheology of intercalated polystyrene/ Na<sup>+</sup>-montmorillonite nanocomposites, *Macromolecular Rapid communication*, 23 2002, 191-195.

Vilsan MN, Meghea A, Sonmez M, Georgescu M, Dynamically cured hybrid polymer nanocomposite based on polypropylene and EPDM rubber, *University Politechnica of Bucharest Scientific Bulletin Series B*, 77, 2015, 165-174.